

Supplementary Information

Polarization-based Colour Tuning of Mixed Colloidal Quantum-Dot Thin Films using Direct Patterning

Eva De Leo,^a Aurelio Rossinelli,^a Patricia Marqués-Gallego,^a Lisa Poulidakos,^a David J. Norris^a and Ferry Prins^{a,b}*

- a. Optical Materials Engineering Laboratory, ETH Zurich, Leonhardstrasse 21, 8092 Zürich, Switzerland*
- b. Condensed Matter Physics Center (IFIMAC), Universidad Autonoma de Madrid, Calle Francisco Tomas y Valiente 6, 28049 Madrid, Spain.*

AUTHOR INFORMATION

Corresponding Author

* Email: ferry.prins@uam.es

1. Scanning-Electron microscopy of concentric grating structures.

In Figure S1, high resolution scanning-electron microscopy (SEM) images of the central sections of the concentric hexagonal and rectangular grating structures are presented.

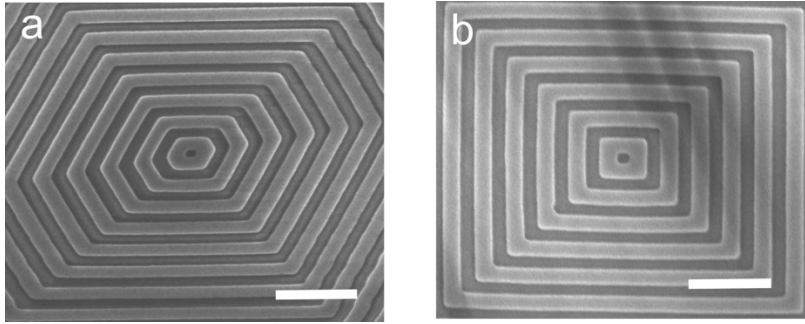


Fig. S1 (A) SEM image of the concentric hexagonal structure presented in the main text (Fig 4b). (B) SEM image of the concentric rectangle structure presented in the main text (Fig. 3a). Scale bars in both panels are $1\mu\text{m}$.

2. Design of rectangular concentric grating array.

In Figure S2, a zoom in of the design of the concentric rectangular grating array is presented, illustrating the grating arrangement at the interface of green and red emitting sections.

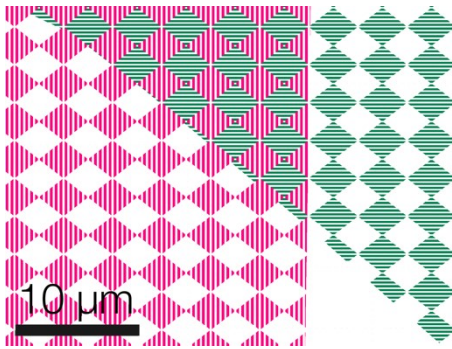


Fig. S2 Detail of the design of the array of rectangular concentric gratings presented in Fig. 3c, illustrating the separation of colors at the interfaces of the different figures.

3. Quantification of the emission enhancement in the surface normal direction.

To quantify the outcoupling efficiency in the out-of-plane direction, we performed k-space imaging of the different grating structures in the RG and RGB films and used a fit of superimposed Gaussians to separate the contributions from the different colors in the emission profile. Figure S3 shows the angle resolved intensity of the rectangular grating for the red outcoupling ($\lambda = 400\text{ nm}$) in S3a and the green outcoupling ($\lambda = 340\text{ nm}$) in S3b. The intensity profiles are normalized to the non-resonant background of the film, thereby accounting for the increased volume of cQDs of the grating structures as compared to the flat film. The enhancement of the outcoupling efficiency along the surface normal direction are extracted from Gaussian fits and reaches as high as 86% for the resonant red emission and 71% for the resonant green emission.

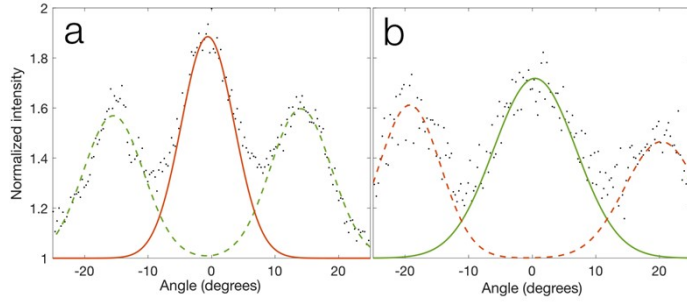


Fig. S3 (A) Angular emission profile of the $\Lambda = 400$ nm grating of the rectangular structure presented in Figure 3. The solid red line indicates the result of the fitting of the central red emission peak, while the dashed green line represents the double Gaussian fit to the side lobes of the green emission. (B) Angular emission profile of the $\Lambda = 340$ nm grating of the same rectangular structure. The solid green line indicates the result of the fitting of the central green emission peak, while the dashed red line represents the double Gaussian fit to the side lobes of the red emission.

Similarly, figure S4 shows the angle resolved intensity of the hexagonal grating in the RGB films for the red outcoupling ($\Lambda = 400$ nm) in S4a, the green outcoupling ($\Lambda = 340$ nm) in S4b and the blue outcoupling ($\Lambda = 275$ nm) in S4c. The enhancement of the outcoupling efficiency in the direct out-of-plane direction extracted from the Gaussian fits reaches 75% for the red emission, 64% for the green emission, and 38% for the resonant blue emission.

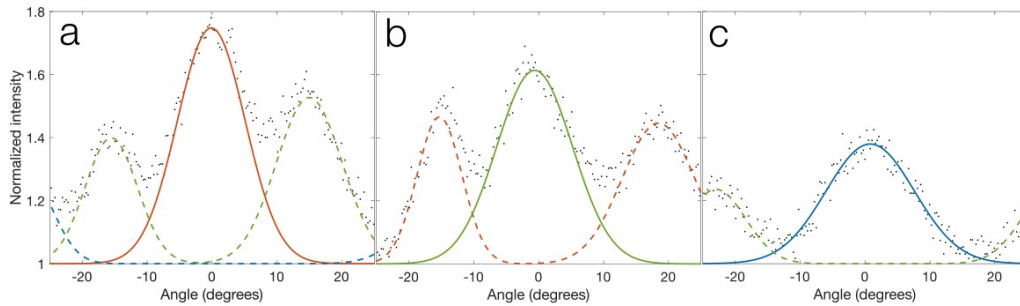


Fig. S4 (A) Angular emission profile of the $\Lambda = 400$ nm grating of the hexagonal structure presented in Figure 4. The solid red line indicates the result of the fitting of the central red emission peak, while the dashed green and blue lines represents the double Gaussian fits to the side lobes of the green and blue emission. (B) Angular emission profile of the $\Lambda = 340$ nm grating of the same hexagonal structure with the solid green line indicating the result of the fitting of the central green emission peak, while the dashed red line represents the double Gaussian fit to the side lobes of the red and blue emission. Please note that for this periodicity, the angular profile of the red and green emission are overlapping. For simplicity, a double Gaussian fit was used for the side lobes. (C) Angular emission profile of the $\Lambda = 275$ nm grating of the same hexagonal structure with the solid blue line indicating the result of the fitting of the central blue emission peak, while the dashed green line represents the double Gaussian fit to the side lobes of the green emission. All angular emission profiles are normalized to the non-resonant background of the k-space measurement.

The differences in the efficiencies of outcoupling for the different grating structures can have several origins. The highest efficiencies in the out-of-plane direction are reached for the outcoupling the red emission (S3a and S4a). This highest efficiency is also accompanied with the sharpest angular emission profile, suggesting that the other grating structures may have a grating periodicity that is slightly off-set from the optimal resonant alignment with the emission wavelength. This misalignment of the periodicity and the peak emission wavelength causes a slight splitting of the branches of the dispersion relation, leading to a broadening of the angular profile and a reduction of the peak efficiency in the out-of-plane direction. These broader profiles are clearly visible in figures S3b, S4b, and S4c. Further optimization of the periodicity of the structures could therefore help to improve the efficiencies of the outcoupling. Finally, we would like to note that the k-space measurements are not corrected for the spectral dependence of the efficiency of the camera and the optical path. However, based on the specifications of these components, we estimate the influence of such variations to be less than 10%.”

4. Polarization dependence of the emission spectra of the hexagonal grating.

Using a linear polarizer, the ratios between the different colours of the hexagonal array of Figure 4b can be modulated, with the resulting spectra at different polarizer orientations shown in Figure S5. The limited modulation of the red emission peak is attributed to the smaller surface area of the red grating sections in the array as compared to the blue and green sections.

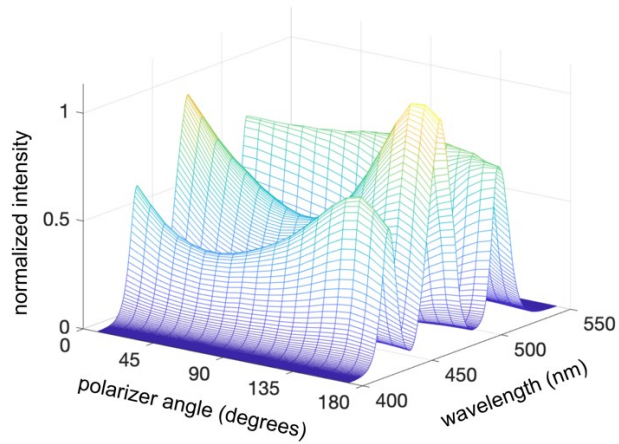


Fig. S5 Polarization dependence of the normalized emission spectrum of the hexagonal concentric grating array presented in Figure 4b.